IEEE Photonics Journal
An IEEE Photonics Society Publication

Impact of Crosstalk on Indoor WDM Optical Wireless Communication Systems

Volume 4, Number 2, April 2012

Ke Wang
Ampalavanapillai Nirmalathas
Christina Lim
Efstratios Skafidas

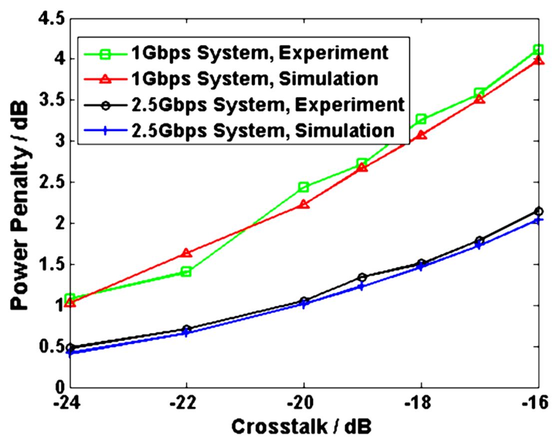

DOI: 10.1109/JPHOT.2012.2188626

IEEE photonics SOCIETY
IEEE

Impact of Crosstalk on Indoor WDM Optical Wireless Communication Systems

Ke Wang,[1,2] Ampalavanapillai Nirmalathas,[1,2] Christina Lim,[2] and Efstratios Skafidas[1,2]

[1]National Information and Communications Technology Australia-Victoria Research Laboratory (NICTA-VRL), Australia
[2]Department of Electrical and Electronic Engineering, The University of Melbourne, Melbourne, Vic. 3010, Australia

DOI: 10.1109/JPHOT.2012.2188626
1943-0655/$31.00 ©2012 IEEE

Manuscript received January 15, 2012; revised February 11, 2012; accepted February 15, 2012. Date of publication March 2, 2012; date of current version March 8, 2012. This work was supported in part by NICTA, which is funded by the Australian Government as represented by the Department of Broadband, Communications, and the Digital Economy and the Australian Research Council through the ICT center of Excellence program. Corresponding author: K. Wang (e-mail: k.wang2@pgrad.unimelb.edu.au).

Abstract: In this paper, we investigate the impact of optical crosstalk on our recently proposed indoor gigabit optical wireless (OW) communication system incorporating wavelength division multiplexing (WDM). A theoretical model that allows this impact to be assessed has been proposed. The analytical results are validated via experiments. We show that the power penalty due to crosstalk in our proposed indoor WDM OW system is lower compared to that in the conventional optical fiber communication systems. In addition, it is found that the power penalty due to crosstalk is lower for the higher speed system since the receiver preamplifier-induced noise dominates the noise process. Finally, the maximum error-free beam footprint for different levels of optical crosstalk has been investigated. The results show that, for the 10- and 12.5-Gb/s systems, the maximum error-free beam footprint is only reduced by ~5 cm, even with comparatively strong crosstalk.

Index Terms: Broadband communications, fiber optics links and subsystems, free space optics, wireless personal area networks, optical crosstalk, wavelength division multiplexing (WDM) technology.

1. Introduction

In the last decade, we have witnessed a rapid development in broadband access technologies in both fixed and mobile network infrastructure [1]. For the deployment of fixed broadband access, passive optical network (PON) technologies have emerged as a popular choice [2]–[4]. In particular, Ethernet PON (EPON) can reduce fiber deployment and maintain an inherently smooth connection with legacy Ethernet networking which is already a mature local area network (LAN) technology deployed ubiquitously in our daily life [3]. On the other hand, wireless LANs (IEEE 802.11) achieves huge commercial success in providing wireless access to end users [5] and WiMax (IEEE 802.16) has also been proposed to provide wider bandwidth, larger coverage area and better quality-of-service (QoS) support [6]. However, their bit rate is highly limited to less than 400 Mb/s. This is because these systems use radio bandwidths of 40 MHz or less in the lower radio frequencies (RFs) in the microwave frequency region, which is already highly congested.

To achieve higher bit rate, millimeter-wave (mm-wave) based systems have sparked a renewed interest in indoor applications to provide mobile communications over a limited area, especially those using the 60-GHz region [7]. For example, a 5-Gb/s mm-wave wireless communication system integrated on a single complementary metal–oxide–semiconductor (CMOS) chip has been successfully achieved by Skafidas *et al.* [8]. However, in this frequency region only ~7 GHz license free bandwidth is available which will ultimately limit the highest communication speed and the mm-wave signals do not propagate well through obstructions such as doors and walls limiting their application to single room deployments [9]. To overcome the limited coverage of the mm-wave systems, radio-over-fiber (ROF) technology, taking advantage of optical fiber distribution networks, has been proposed and widely investigated [10]–[12]. However, such a system requires expensive optoelectronic devices such as high-speed modulator and photodiode (PD) and the performance may be limited by fiber chromatic dispersion.

In contrast to the RF-based technologies, the use of infrared radiation for indoor wireless communications has also been considered [13]–[16]. Although there are some limitations such as the line-of-sight (LOS) transmission requirement and the limited transmission power due to laser eye and skin safety regulations [17], there are even more advantages including the availability of large unregulated bandwidth resource and free of interference from the surrounding electromagnetic signals [18]. Therefore, it can be used in the RF hostile environments such as hospitals. Furthermore, since in optical wireless (OW) communication systems the optical carrier is modulated by baseband data, the signal distribution is simpler and expensive high-speed optoelectronics devices are no longer needed.

There are generally two kinds of indoor OW communication systems, namely the conventionally LOS system and the diffused beam system [13], [19]–[22]. In previous studies, we combined the advantages of these two systems and proposed a novel indoor OW communication system [23]–[26]. The OW technique is incorporated with localization function and the ceiling mounted fiber end serves as the transmitter. The fiber transmitter is composed of a fiber end, a lens and a steering mirror [23]. The lens is used to increase the divergence of the signal beam to cover a certain area for limited mobility purpose and the steering mirror is used to change the orientation of the light according to the localization information. Then a comparatively wider divergent beam is employed to cover the user's position as well as the surrounding areas. Therefore, high-speed direct LOS link is available for high-speed data transmission and limited mobility over the cover area can be provided. When the user moves out of the area covered by the signal light, which can be identified by the localization system, the steering mirror will change its orientation adaptively to the new position. Through this way mobility as well as high-speed communication can be provided over the entire room. Up to 12.5-Gb/s data transmission with a reasonable error-free beam footprint has been experimentally demonstrated [26]. In addition, we have also demonstrated a novel indoor localization system based on the full-duplex communication capability provided by our OW system [27].

In addition to the single channel system, we have also proposed to incorporate the wavelength division multiplexing (WDM) technology to further increase the overall bit rate [27], [28]. A 4 $\times$ 12.5-Gb/s indoor WDM OW communication system has been experimentally demonstrated by coupling the signal back to the fiber and using the fiber-based demultiplexer (DEMUX). However, in real applications it is more desirable to use the thin-film based free space optical bandpass filters due to their cost-effectiveness through mass production, the capability of tuning the passband by thermal-optic effect, and the easier integration with other components. On the other hand, such optical filters often have a broader passband profile which will introduce optical crosstalk to adjacent channels and the crosstalk mainly results in additive noise [28]. Therefore, this crosstalk will result in a power penalty and in this paper we investigate the impact of optical crosstalk in our proposed OW system both theoretically and experimentally.

The rest of the paper is organized as follows: In Section 2, the theoretical analysis will be described, and the simulation results will be shown and analyzed; in Section 3, the experimental results will be presented and discussed, and finally, in Section 4, conclusions will be given.

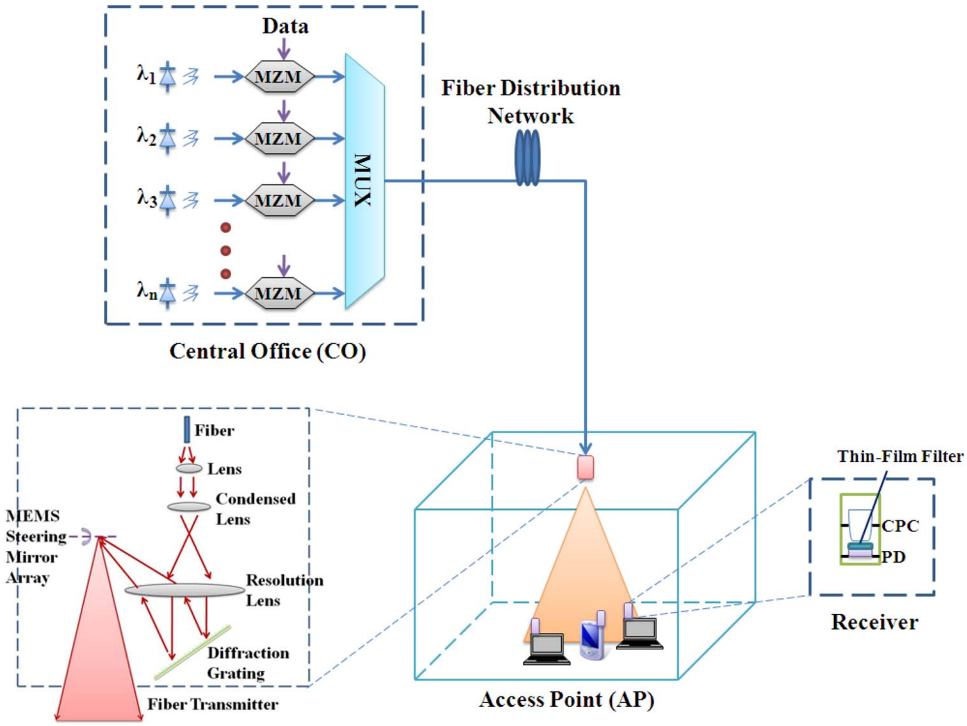

Fig. 1. System architecture.

2. Theoretical Analysis on Crosstalk in Indoor Gigabit OW Communication Systems

2.1. Architecture of Proposed Indoor WDM OW System

The architecture of the previously proposed indoor WDM OW communication system is shown in Fig. 1. Multiple wavelengths are generated and modulated with baseband signal in the central office (CO) and then transmitted to the room/access point (AP) via an optical fiber distribution network. The ceiling mounted fiber end serves as the transmitter so a separate laser source is no longer needed in each room [13]–[15]. Inside the rooms the OW technique is incorporated with the localization function. The localization system provides location information of the users and our recently proposed novel indoor OW localization system is capable of precise localization [26]. The wavelengths are then separated in free space by using an assembly comprised of a diffraction grating and lenses similar to that described in [29]. By controlling lenses the divergence of the signal light can be adjusted to cover a certain area for the purpose of supporting a limited mobility of customers. Different wavelengths are cast onto different MEMS steering mirrors integrated as an array so they can be steered to different positions according to the localization information to serve multiple users. If all of these wavelengths are steered to the same position, ultrabroadband full WDM transmission is realized. At the receiver end the light is collected by a compound parabolic concentrator (CPC) and then detected with a PD. When multiple wavelengths are used to cover the same area, a bandpass filter is needed to reject interference signals as well as to select the desired communication channel. In our system, a thin-film based optical bandpass filter will be used after the CPC because of its simplicity and low-cost feature.

However, in such a WDM OW system crosstalk among different channels may lead to degradation in the receiver sensitivity. To quantify the changes in the receiver sensitivity, we define the receiver sensitivity as the minimum average received power required by the receiver to achieve the target bit-error-rate (BER) $< 10^{-9}$.

2.2. Theoretical Model

In our proposed WDM OW communication system, we use on–off-keying (OOK) modulation format since it is the simplest and most mature technique for OW communication system. The dominant noise processes in single channel OW system are the background light-induced shot noise and the receiver preamplifier-induced noise [13]. Although the signal dependent noise also exists in the system, it is shown in [13] that this noise component is small enough to be neglected. Therefore, the noise variance σ_0^2 and σ_1^2 associated with the transmitted signal "0" and "1" are the same and can be given by

$$\sigma_0^2 = \sigma_1^2 = \sigma^2 = \sigma_{pr}^2 + \sigma_{bn}^2 \tag{1}$$

where σ_{pr}^2 represents the preamplifier-induced noise variance component and σ_{bn}^2 represents the background light-induced shot noise variance.

The preamplifier used in our system is a field-effect transistor (FET) transimpedance receiver proposed in [30]. The principle noise sources in this preamplifier are thermal noise associated with the FET channel conductance, and the load and the feedback resistors, shot noise arising from gate leakage current and $1/f$ noise. The preamplifier shot noise variance is given by [30]

$$\sigma_{pr}^2 = \left(\frac{4kT}{R_F} + 2eI_L\right) I_2 B + \frac{4kT\Gamma}{g_m}(2\pi C_T)^2 A_F f_c B^2 + \frac{4kT\Gamma}{g_m}(2\pi C_T)^2 I_3 B^3 \tag{2}$$

where B is the electrical bandwidth, A_F is the weighting function and for the not-return-to-zero (NRZ) coding format $A_F = 0.184$, I_L is the total leakage current (FET gate current and dark current of PD), g_m is the FET transconductance, $\tilde{A}$ is a noise factor associated with channel thermal noise and gate-induced noise in the FET, C_T is the total input capacitance consisting of PD and stray capacitance, f_c is the $1/f$ corner frequency of the FET, I_2 and I_3 are the weighting functions which are dependent only on the input optical pulse shape to the receiver and the equalized output pulse shape ($I_2 = 0.562$ and $I_3 = 0.0868$ [30]), R_F is the feedback resistance, k is the Boltzmann's constant, T is the absolute temperature, and e is the electron charge.

For simplicity, the FET gate leakage and $1/f$ noise can be neglected [30]. Therefore, the preamplifier-induced noise variance is simplified to

$$\sigma_{pr}^2 = \frac{4kT}{R_F} I_2 B + \frac{4kT\Gamma}{g_m}(2\pi C_T)^2 I_3 B^3. \tag{3}$$

In addition to the preamplifier-induced noise, the background light-induced shot noise can be calculated as

$$\sigma_{bn}^2 = 2eRP_{bn} I_2 B \tag{4}$$

where R is the responsivity of the PD (R is supposed to be 0.8 A/W in this paper), and P_{bn} is the received background light power. This background light originates from the lamps inside the room and here we assume six 100 W tungsten floodlights to create a well-illuminated environment. These lamps can be modeled as generalized Lambertian sources [31], and the radiant intensity (W/Sr) is

$$I(\varphi) = \frac{n+1}{2\pi} \times P_t \times \cos^n(\varphi) \tag{5}$$

where P_t is the total transmitted optical power radiated by the lamp, φ is the angle of incidence with respect to the transmitter's surface normal, and n is the mode number describing the shape of the transmitted beam. For our system, the lamp has a mode $n = 2.0$ and optical spectral density of $P_{\text{lamp}} = 0.037$ W/nm [31]. To reduce the received background light power, an optical bandpass filter based on thin film is utilized in front of the concentrator at the receiver end.

Therefore, when the concentrator area is $R_{receiver}$, the received background light power in (4) is given by

$$P_{bn} = \sum_{i=1}^{4} \frac{n+1}{2\pi} \times P_{lamp} \times \cos^n(\varphi_i) \times B_{filter} \times R_{receiver}. \quad (6)$$

The performance of the OW link can be quantified by the received signal-to-noise ratio (SNR) and it is defined for a single channel as [13]

$$\text{SNR} = \left(\frac{R \times (P_{s1} - P_{s0})}{\sigma_0 + \sigma_1}\right)^2 \quad (7)$$

where P_{s0} and P_{s1} are the powers associated with signal "0" and "1," respectively, and $P_{s0} - P_{s1}$ accounts for the eye opening at the sampling instant.

For the WDM OW system, since the crosstalk is almost a random uncorrelated process and the PD is a square-law device, the original signal will beat with the interference signal and the resulting photocurrent will be

$$i(t) \propto |E_1 + E_2|^2 = |e_1|^2 + |e_2|^2 + 2|e_1 \cdot e_2| \cdot \cos[(\omega_1 - \omega_2)t + (\varphi_1(t) - \varphi_2(t))] \quad (8)$$

where E_1 is the total electric field from the original signal, e_1 is the vector amplitude, ω_1 is its optical frequency, and $\varphi_1(t)$ is its phase which might change with time. Analogous notation is used for the interference signal (signal 2). The impact of crosstalk on the system can be seen as an additional noise and from [32] it is found that this noise variance can be given by

$$\sigma_{XT}^2 = 4kR^2\xi\overline{P}^2, \qquad k = \begin{cases} 1, & \text{dispersive crosstalk} \\ 2, & \text{nondispersive crosstalk} \end{cases} \quad (9)$$

where ξ is the ratio of crosstalk power to the original signal power and $\overline{P}^2$ is the average received optical signal power. The dispersive crosstalk is defined as the crosstalk that results from a continuum of interference paths all having slightly different propagation delays, such that all intensity modulation of the signal generating the crosstalk is averaged out. The nondispersive crosstalk refers to an interference path in which the NRZ modulation of the data stream is largely preserved and the maximum signal power is twice the average [32]. In our proposed system, the original signal and interference signal all originate from the ceiling mounted fiber transmitter so the crosstalk is nondispersive. Therefore, the noise variance in the WDM OW system is given by

$$\sigma_0^2 = \sigma_1^2 = \sigma^2 = \sigma_{pr}^2 + \sigma_{bn}^2 + \sigma_{XT}^2. \quad (10)$$

To achieve the same SNR as in a single channel system, a larger received power is required in the WDM system because of the crosstalk. Here, we define the difference in the required received power as the crosstalk power penalty, and it can be calculated as

$$\text{Power} - \text{Penalty (dB)} = 5 \times \log_{10} \frac{\sigma_{pr}^2 + \sigma_{bn}^2 + \sigma_{XT}^2}{\sigma_{pr}^2 + \sigma_{bn}^2}. \quad (11)$$

2.3. Simulation Results

Based on (1)–(11), we analyze and quantify the impact of crosstalk on the performance of our proposed OW system. The room considered in the simulation is a medium sized 5 m × 4 m × 3 m room with a real office scenario, as shown in Fig. 2. The room is divided into two equal sized rectangular cubicles (2.5 m × 3 m × 3 m), and it is equipped with six strong background lamps to create a well-illuminated environment (∼550 lx illumination) [33], [34]. The positions of the six lamps are (1.25, 1, 3), (2.5, 1, 3), (3.75, 1, 3), (1.25, 3, 3), (2.5, 3, 3), and (3.75, 3, 3), respectively. In addition, the cubicle partitions are opaque so all the signal incident on them are either absorbed or blocked. Therefore, physical shadowing exists in considerable areas inside the room. To overcome

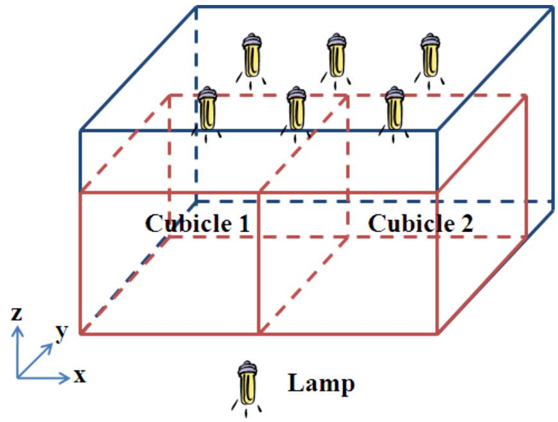

Fig. 2. Simulated room structure.

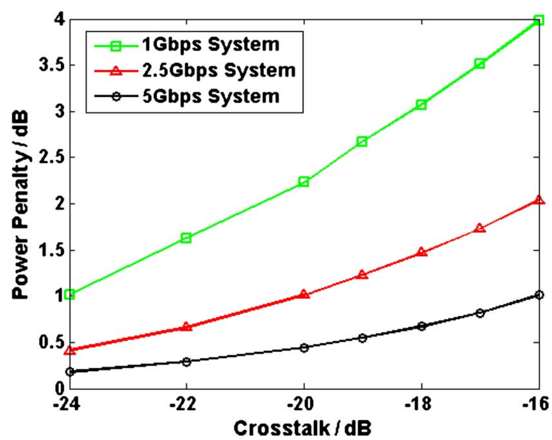

Fig. 3. Simulation results on power penalty due to crosstalk.

this problem, the fiber transmitter is installed just above the intersections of the two cubicles and in the coordinates shown in Fig. 2, the location of the fiber transmitter is (2.5, 3, 3). It should be noted that the position of the fiber transmitter is the same as one of the illumination lamps. However, since the fiber transmitter and small in size, in real applications it is still feasible. Furthermore, the wavelength used for the high-speed OW communications is in the 1550-nm band while the spectrum of the lamps is mainly within the visible band. Therefore, there will be negligible interference.

In the simulation, the electrical bandwidth B of the PD is supposed to be equal to the bit rate of the system and in the experiment, this can be achieved by adding corresponding electrical bandpass filter after signal detection with PD. Furthermore, the passband of the optical bandpass filter is chosen to be 10 nm to make sure that the signal under investigation can always pass through the filter at any possible incident angle. In addition, the transmission power of the signal under investigation is fixed at 7 mW, the maximum possible power due to laser eye and skin safety regulations [17]. At the receiver end, the field-of-view (FOV) of the CPC is supposed to be 45°.

Fig. 3 shows the theoretical results of power penalty due to crosstalk when the user is at the position of (1.25, 1, 1), which is just under a strong background lamp for different transmission bit rates. The received background light power is ~ -26.13 dBm, and the crosstalk level changes from -16 dB to -24 dB. The crosstalk level is defined as the ratio of the received interference signal power to the received power of the signal under investigation. The bit rates under investigation are 1, 2.5, and 5 Gb/s, respectively. From Fig. 3 it is clear the power penalty increases with crosstalk.

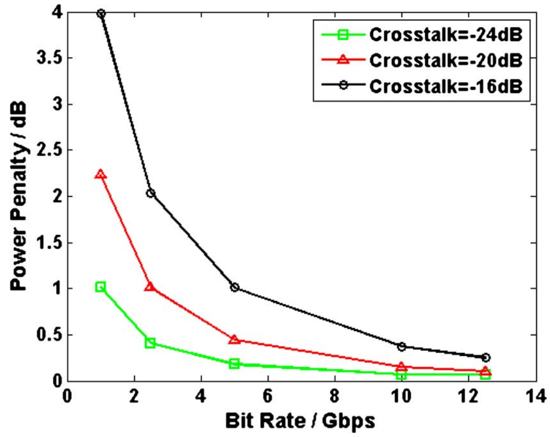

Fig. 4. Power penalty with respect to bit rate for different levels of crosstalk (simulation results).

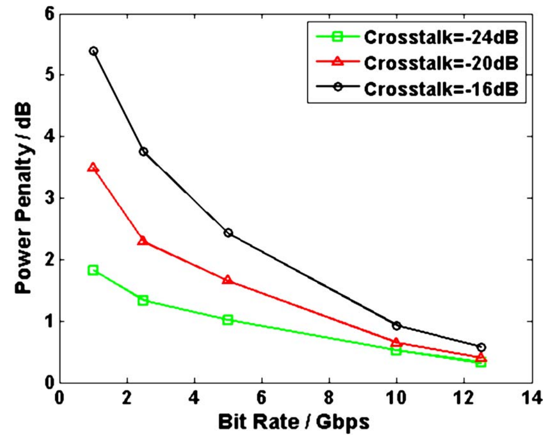

Fig. 5. Simulation results on power penalty due to crosstalk for different communication bit rates at the position of (4.5, 0.5, 1).

Furthermore, when the crosstalk power is comparatively small, the power penalty increases almost linearly with the crosstalk level. However, when the crosstalk is larger the power penalty increases much faster. In addition, for the same level of crosstalk, lower speed system incurs a larger power penalty. This is due to the fact that at lower bit rate, the receiver preamplifier noise is negligibly small while the background noise is constant. Therefore, the impact of crosstalk-induced noise becomes dominant which induces a larger power penalty, as shown in Fig. 3. To show this phenomenon more clearly, in Fig. 4 we summarize the power penalty with respect to bit rates for the same level of crosstalk. From Fig. 4, we can see that the impact of crosstalk is more pronounce for the lower speed system and is almost negligible for higher bit rates. At higher bit rates, the preamplifier noise dominates the noise processes. It should be noted that although the power penalty is higher for lower speed system, it does not mean that the proposed system is not suitable when the speed is low. For lower speed system, the receiver sensitivity is much better than the higher speed system due to the smaller preamplifier noise. Therefore, the power budget is not as tight as that in the higher bit rate system and a slightly higher power penalty due to crosstalk is not a critical issue.

When the user is at the position of (4.5, 0.5, 1), which is further away from the overhead lamps, the power penalty due to crosstalk is shown in Fig. 5. In this case the received background light power is ~ -30.27 dBm. It is obvious that for the same bit rate and crosstalk level, the power penalty due to crosstalk is higher in the position where the received background light power is

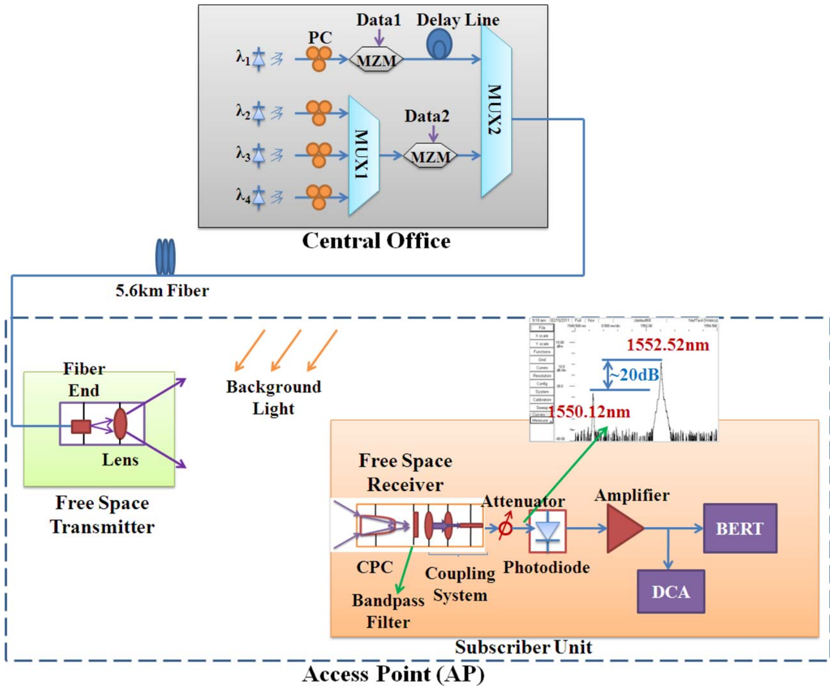

Fig. 6. Experiment setup.

smaller. This is because when the background light-induced shot noise is smaller, the impact of crosstalk becomes more prominent.

3. Experiments and Discussions

To verify the theoretical analysis and simulation on the power penalty due to crosstalk in the WDM OW communication system, we have also carried out experiments and the setup is shown in Fig. 6. The setup is similar to that used in [28]. Four wavelengths are generated, modulated and multiplexed in the CO. The wavelength under investigation is modulated with one PRBS data $(2^{31}-1)$ and the other three are first multiplexed and then modulated with another $2^{31}-1$ PRBS data. These two PRBS data are generated with the same pulse pattern generator (PPG) due to our device limitations. To decorrelate these data, an optical delay line with a length of $\sim$250 m is utilized. The wavelengths used here ranges from 1550.12 nm to 1552.52 nm with a fixed 100 GHz channel spacing. The four modulated signals are transmitted to the AP via an optical fiber distribution network and it is emulated by the 5.6 km standard single-mode fiber in the experiment. Then the signals exit the fiber end and pass through a lens to increase its divergence before propagating in the free space. At the receiver end the signals are collected by a CPC with a FOV of 45°. The signals are then coupled into the fiber with a coupling system consisting of multiple lens and fiber collimator before detection using a small photosensitive area fiber coupled PD (65 μm $\times$ 65 μm). Although using a large photosensitive area PD just after the CPC can make this system much simpler, due to device limitations we choose to use the coupling system and a small PD. The 3-dB electrical bandwidth of this PD is $\sim$11.5 GHz, and the responsivity is $\sim$0.84 A/W at 1550 nm. This PD is integrated with a TIA and the sensitivity at 12.5 Gb/s and BER $< 10^{-9}$ is ~ -20.7 dBm (without background light and with $\sim$16 dB extinction ratio of the transmitter signal). The detected signals are then amplified and measured with a BER tester (BERT) and wide-bandwidth digital communication analyzer (DCA).

It should be noted that, in real applications it is difficult to employ such a dense WDM system since the passband of the thin-film based filter is normally broad. In addition, the passband of the filter also depends on the incident angle, so in some cases the signal may be filtered out with such

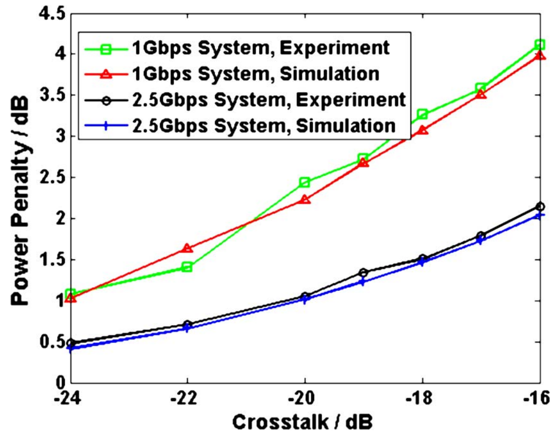

Fig. 7. Power penalty due to crosstalk for 1- and 2.5-Gb/s systems. Both experimental results and simulation results are shown.

narrow channel spacing. However, for proof-of-concept demonstration the use of dense WDM is still acceptable. This is because the interference signal acts like noise which is not dependent on the wavelength and in the experiment the incident angle of the signal is always fixed. We choose this dense channel spacing here due to the availability of low-cost fiber-based multiplexer (MUX) and standard WDM laser source. In addition, the transmission power of the signal under investigation is fixed at 7 mW, the maximum safe power due to laser eye and skin safety regulations [17].

In the experiment, a free space optical bandpass filter is used at the subscriber unit. This filter is a multicavity Fabry–Perot or etalon based one and has a full-width at half-maximum (FWHM) passband of $\sim$10 nm. By changing the output power of the interference signal at the laser side, different levels of crosstalk can be experimentally emulated. Shown in the inset of Fig. 6 is the optical spectrum when the crosstalk is ~ -20 dB and here we only turn on one interference signal for easier measurement of crosstalk level. The wavelength under investigation is 1552.52 nm and the wavelength introducing crosstalk is 1550.12 nm. In addition, the polarization of both signals is not controlled to emulate the random situation in real applications. The experimental results for the power penalty due to crosstalk for 1- and 2.5-Gb/s systems are shown in Fig. 7. A variable optical attenuator is used before the PD to measure the receiver sensitivity. The crosstalk ξ changes from -16 dB to -24 dB and simulation results based on the parameters used in the experiments are also shown. The received background light power is measure to be ~ -25.96 dBm. It is obvious that the experimental results agree well with those obtained through the simulation and this verifies the feasibility of our theoretical model. Furthermore, the power penalty from the experiments is always slightly larger than that from the model. This is due to the slightly lower received background light power in the experiment.

Fig. 8 shows the experimental results on power penalty with respect to transmission bit rate. The results when the crosstalk level ξ is -22 dB and -18 dB are shown in Fig. 8(a) and (b), respectively. In this investigation, the direct lamps are turned on and off, and the received background light powers are -26.13 dBm and -31.07 dBm, respectively. It can be seen from both figures that the theoretical results always agree well with the experimental results. The difference is well within 0.3 dB and these results validate our proposed model. Furthermore, for the 12.5-Gb/s system, when the crosstalk level is -18 dB and the direct lamps are turned off, the power penalty is only $\sim$0.5 dB. This power penalty will result in the reduction in the error-free beam footprint. Therefore, we have also carried out experiments to investigate the change in error-free beam footprint due to crosstalk.

Shown in Fig. 9 is the maximum error-free beam footprint of the 10-Gb/s system and 12.5-Gb/s system for different crosstalk level ξ. Without crosstalk, when the transmission power is 7 mW, the maximum error-free beam footprint is 79.2 cm and 76.4 cm, respectively [28]. It is clear that when the crosstalk level ξ is -24 dB, there is only a 0.6-cm and 0.5-cm reduction in the maximum error-free beam footprint for 10 Gb/s and 12.5 Gb/s, respectively. Even when the crosstalk level ξ is

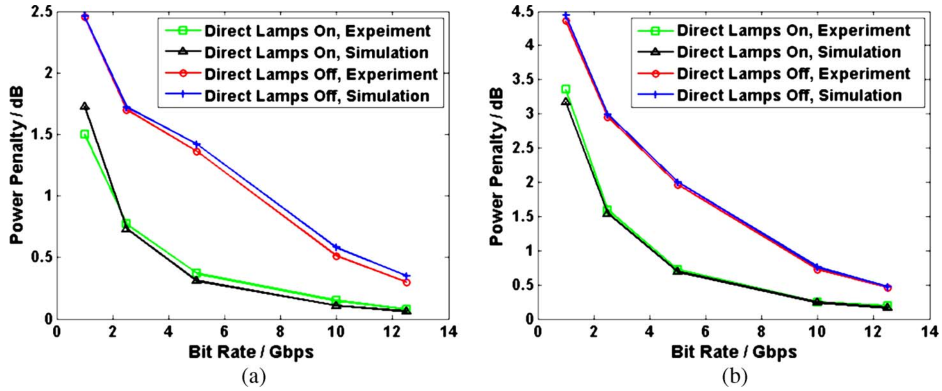

Fig. 8. Power penalty with respect to bit rate. Both experimental and simulation results are shown. (a) −22-dB crosstalk and (b) −18-dB crosstalk.

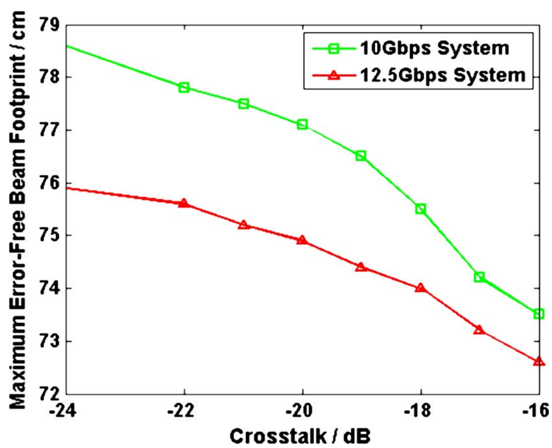

Fig. 9. Maximum error-free beam footprint with respect to crosstalk. Both 10-Gb/s and 12.5-Gb/s systems are investigated.

−16 dB, the reduction is ∼5.7 cm and ∼3.8 cm and a reasonable beam footprint (> 70 cm) can always be achieved. Therefore, although the usage of low- cost thin film based optical bandpass filter which has a wider bandwidth will induce some crosstalk and power penalty, it is still feasible to achieve high-speed OW communication with limited footprint. When this system is incorporated with the localization system, error-free operation as well as mobility can be provided over the entire room.

4. Conclusion

In this paper, we investigate the impact of optical crosstalk on indoor WDM OW communication system. The crosstalk is mainly introduced by the imperfect thin-film based bandpass filter used in the system. A theoretical model that allows this impact to be assessed has been proposed and validated via experiments. The simulated results show that for a fixed level of crosstalk, the resultant power penalty is smaller for a higher speed system. This is mainly because for higher speed system the preamplifier-induced noise is dominant. Furthermore, the power penalty due to optical crosstalk is larger when the received background light power is smaller.

In addition to the theoretical study, verification experiments have also been carried out and the experimental results agree well with the simulated ones. Furthermore, the maximum error-free beam footprint at different levels of optical crosstalk has been investigated. The results show that for high-speed systems the reduction in error-free beam footprint is always smaller than 6 cm even with strong optical crosstalk and for the 12.5-Gb/s system a reasonable beam footprint of $>$ 72 cm can still be achieved.

References

[1] R. Heron, "Next generation optical access networks," in *Proc. Adv. Photon. Congr.*, Toronto, ON, Canada, 2011, p. AMA2.
[2] M. Daneshmand, C. Wang, and W. Wei, "Advances in passive optical networks," *IEEE Commun. Mag.*, vol. 49, no. 2, pp. s12–s14, Feb. 2011.
[3] J. Zhang and N. Ansari, "Toward energy-efficient 1G-EPON and 10G-EPON with sleep-aware MAC control and scheduling," *IEEE Commun. Mag.*, vol. 49, no. 2, pp. s33–s38, Feb. 2011.
[4] K. Y. Cho, B. S. Choi, Y. Takushima, and Y. C. Chung, "25.78-Gb/s operation of RSOA for next-generation optical access networks," *IEEE Photon. Technol. Lett.*, vol. 23, no. 8, pp. 495–497, Apr. 2011.
[5] H. Singh, J. Hsu, L. Verma, S. S. Lee, and N. Chiu, "Green operation of multi-band wireless LAN in 60 GHz and 2.4/5 GHz," in *Proc. IEEE CCNC*, Las Vegas, NV, 2011, pp. 787–792.
[6] K. Lu, Y. Qian, and H.-H. Chen, "Wireless broadband access: WiMax and beyond—A secure and service-oriented network control framework for WiMax networks," *IEEE Commun. Mag.*, vol. 45, no. 5, pp. 124–130, May 2007.
[7] C. Liu, E. Skafidas, and R. Evans, "Capacity and data rate for millimeter wavelength systems in a short range package radio transceiver," *IEEE Trans. Wireless Commun.*, vol. 9, no. 3, pp. 903–906, Mar. 2010.
[8] B. Yang, Y. Mo, K. Wang, Y. Feng, B. Wicks, C. M. Ta, F. Zhang, Z. Liu, C. Liu, G. Felic, P. Nadagouda, T. Walsh, and E. Skafidas, "Implementation of a Gigabit per second millimeter wave transceiver on CMOS," in *Proc. 2nd Int. Conf. Wireless Broadband Ultra Wideband Commun.*, Sydney, Australia, 2007, pp. 71–74.
[9] E. Skafidas, F. Zhang, B. Yang, B. Wicks, Z. Liu, T. C. Minh, Y. Mo, K. Wang, G. Felic, P. Nadagouda, T. Walsh, W. Shieh, I. Mareels, and R. Evans, "A 60 GHz transceiver on CMOS," in *Proc. Int. Top. Meet. Microw. Photon.*, Sydney, Australia, 2008, pp. 306–309.
[10] A. Islam, M. Bakaul, A. Nirmalathas, and G. E. Town, "Millimeter-wave radio-over-fiber system based on heterodyned unlocked light sources and self-homodyne RF receiver," *IEEE Photon. Technol. Lett.*, vol. 23, no. 8, pp. 459–461, Apr. 2011.
[11] Y.-T. Hsueh, H.-C. Chien, A. Chowdhury, J. Yu, and G.-K. Chang, "Performance assessment of radio links using millimeter-wave over fiber technology with carrier suppression through modulation index enhancement," *IEEE/OSA J. Opt. Commun. Netw.*, vol. 3, no. 3, pp. 254–258, Mar. 2011.
[12] C. Lim, A. Nirmalathas, M. Bakaul, P. Gamage, K.-L. Lee, Y. Yang, D. Novak, and R. Waterhouse, "Fiber-wireless networks and subsystem technologies," *J. Lightw. Technol.*, vol. 28, no. 4, pp. 390–405, Feb. 2010.
[13] J. M. Kahn and J. R. Barry, "Wireless infrared communications," *Proc. IEEE*, vol. 85, no. 2, pp. 265–298, Feb. 1997.
[14] F. R. Gfeller and U. Bapst, "Wireless in-house data communication via diffuse infrared radiation," *Proc. IEEE*, vol. 67, no. 11, pp. 1474–1486, Nov. 1979.
[15] J. R. Barry, J. M. Kahn, W. J. Krause, E. A. Lee, and D. G. Messerschmitt, "Simulation of multipath impulse response for indoor wireless optical channels," *IEEE J. Select. Areas Commun.*, vol. 11, no. 3, pp. 367–379, Apr. 1993.
[16] M. Alresheedi and J. M. H. Elmirghani, "Performance evaluation of 5 Gbit/s and 10 Gbit/s mobile optical wireless systems employing beam angle and power adaptation with diversity receivers," *IEEE J. Sel. Commun.*, vol. 29, no. 6, pp. 1328–1340, Jun. 2011.
[17] *Safety of Laser Products—Standards Australia International Ltd and Standards New Zealand*, AS/NZS 2211.1:2004, 2004.
[18] J. M. Kahn, J. R. Barry, M. D. Audeh, J. B. Carruthers, W. J. Krause, and G. W. Marsh, "Non-directed infrared links for high-capacity wireless LANs," *IEEE Pers. Commun.*, vol. 1, no. 2, pp. 12–25, 1994.
[19] A. G. Al-Ghamdi and J. M. H. Elmirghani, "Spot diffusing technique and angle diversity performance for high speed indoor diffuse infra-red wireless transmission," *Proc. Inst. Elect. Eng.—Optoelectron.*, vol. 151, no. 1, pp. 46–52, Feb. 2004.
[20] P. Djahani and J. M. Kahn, "Analysis of infrared wireless links employing multibeam transmitters and imaging diversity receivers," *IEEE Trans. Commun.*, vol. 48, no. 12, pp. 2077–2088, Dec. 2000.
[21] S. T. Jovkova and M. Kavehard, "Multispot diffusing configuration for wireless infrared access," *IEEE Trans. Commun.*, vol. 48, no. 6, pp. 970–978, Jun. 2000.
[22] M. R. Pakravan, E. Simova, and M. Kavehrad, "Holographic diffusers for indoor infrared communication systems," *Int. J. Wireless Inf. Netw.*, vol. 4, no. 4, pp. 259–274, Oct. 1997.
[23] K. Wang, A. Nirmalathas, C. Lim, and E. Skafidas, "High speed duplex optical wireless communication system for indoor personal area networks," *Opt. Exp.*, vol. 22, no. 24, pp. 25 199–25 216, Nov. 2010.
[24] K. Wang, A. Nirmalathas, C. Lim, and E. Skafidas, "Indoor gigabit optical wireless communication system for personal area networks," in *Proc. 23rd IEEE PHO*, Denver, CO, 2010, pp. 224–225.
[25] K. Wang, A. Nirmalathas, C. Lim, and E. Skafidas, "Gigabit optical wireless communication system for indoor applications," in *Proc. ACP Conf. Exhib.*, Shanghai, China, 2010, pp. 453–454.
[26] K. Wang, A. Nirmalathas, C. Lim, and E. Skafidas, "High-speed optical wireless communication system for indoor applications," *IEEE Photon. Technol. Lett.*, vol. 23, no. 8, pp. 519–521, Apr. 2011.
[27] K. Wang, A. Nirmalathas, C. Lim, and E. Skafidas, "4 $\times$ 12.5 Gbps WDM optical wireless communication system for indoor applications," *J. Lightw. Technol.*, vol. 29, no. 13, pp. 1988–1996, Jul. 2011.
[28] P. J. Legg, M. Tur, and I. Andonovic, "Solution paths to limit interferometric noise induced performance degradation in ASK/direct detection lightwave networks," *J. Lightw. Technol.*, vol. 14, no. 9, pp. 1943–1954, Sep. 1996.

[29] D. M. Marom, D. T. Neilson, D. S. Greywall, C.-S. Pai, N. R. Basavanhally, V. A. Aksyuk, D. O. Lopez, F. Pardo, M. E. Simon, Y. Low, P. Kolodner, and C. A. Bolle, "Wavelength-selective 1 $\times$ K switches using free-space optics and MEMS micromirrors: Theory, design, and implementation," *J. Lightw. Technol.*, vol. 23, no. 4, pp. 1620–1630, Apr. 2005.
[30] B. Leskovar, "Optical receivers for wide band data transmission systems," *IEEE Trans. Nucl. Sci.*, vol. 36, no. 1, pp. 787–793, Feb. 1989.
[31] J. B. Carruthers, "Multipath channels in wireless infrared communications: Modeling, angle diversity and estimation," Ph.D. dissertation, Univ. California, Berkeley, CA, 1997.
[32] M. J. Yadlowsky and V. L. da Silva, "Experimental comparison of the effect of discrete and distributed path inband crosstalk on system performance: Application to predicting," *J. Lightw. Technol.*, vol. 16, no. 10, pp. 1813–1821, Oct. 1998.
[33] *Interior and Workplace Lighting—General Principles and Recommendations*, AS1680.1-2006, 2006.
[34] *Interior and Workplace Lighting—Specific Applications*, AS/NZS 1680.2 series, 2008.